

This article is dedicated to Professor Satoshi Ōmura in celebration of his 2015 Nobel Prize.

## Regular Article

## In Situ Click Chemistry for the Identification of a Potent D-Amino Acid Oxidase Inhibitor

Shohei Toguchi,<sup>a</sup> Tomoyasu Hirose,<sup>a,b</sup> Kazuko Yorita,<sup>c</sup> Kiyoshi Fukui,<sup>c</sup> K. Barry Sharpless,<sup>d</sup> Satoshi Ōmura,<sup>\*b</sup> and Toshiaki Sunazuka<sup>\*a,b</sup>

<sup>a</sup>Graduate School of Infection Control Sciences, Kitasato University; 5–9–1 Shirokane, Minato-ku, Tokyo 108–8641, Japan; <sup>b</sup>The Kitasato Institute for Life Sciences, Kitasato University; 5–9–1 Shirokane, Minato-ku, Tokyo 108–8641, Japan; <sup>c</sup>Institute for Enzyme Research, Tokushima University; 3–18–15 Kuramotocho, Tokushima 770–8503, Japan; and <sup>d</sup>Department of Chemistry, The Scripps Research Institute; 10550 North Torrey Pines Road, La Jolla, CA 92037–1000, U.S.A..

Received November 3, 2015; accepted November 10, 2015; advance publication released online December 18, 2015

**In situ click chemistry is a target-guided synthesis approach for discovering novel lead compounds by assembling organic azides and alkynes into triazoles inside the affinity site of target biogenic molecules such as proteins. We report *in situ* click chemistry screening with human D-amino acid oxidase (hDAO), which led to the identification of a more potent hDAO inhibitor. The hDAO inhibitors have chemotherapeutic potential as antipsychotic agents. The new inhibitor displayed competitive inhibition of hDAO and showed significantly increased inhibitory activity against hDAO compared with that of an anchor molecule of *in situ* click chemistry.**

**Key words** fragment-based lead discovery; templated reaction; ligand-binding site; drug discovery; triazole formation; ligand affinity

Although D-amino acids exist in a wide range of organisms, they are nonetheless often called unnatural amino acids. D-Serine is abundant in the forebrain and acts as an endogenous co-agonist of N-methyl-D-aspartate (NMDA) receptors to enhance neurotransmission.<sup>1)</sup> D-Amino acid oxidase (DAO) was the first flavoenzyme to be identified, in 1935 by Krebs,<sup>2)</sup> and catalyzes the oxidative deamination reaction of D-amino acids. This reaction by human DAO (hDAO) in the brain primarily converts D-serine to hydroxypyruvate to regulate the concentration of D-serine. The overexpression of hDAO in the brain therefore causes neuropsychiatric disorders such as schizophrenia, a serious public health problem that affects nearly 0.8% of the global population, by reducing the amount of D-serine below the level required for adequate neuronal function.<sup>3,4)</sup> Furthermore, a protein from the human gene G72 has been identified as an interacting partner to activate hDAO, and the association of both DAO and gene G72 with schizophrenia together with activation of hDAO activity by a G72 protein product points to the involvement of the regulation of

NMDA receptor.<sup>5)</sup> Thus, hDAO inhibitors have potential to be lead compounds to the development of therapeutic agents for schizophrenia.

Within the realm of click chemistry research, triazole formation between organic azide and alkyne is widely recognized. Triazole formation includes the 1,3-dipolar reaction known as the Huisgen cycloaddition,<sup>6–9)</sup> and catalytic reactions that selectively afford the corresponding 1,4-substituted triazole or 1,5-substituted triazole using monovalent copper<sup>10,11)</sup> or ruthenium reagents,<sup>12,13)</sup> respectively. *In situ* click chemistry is a target-guided synthesis (TGS) method for the fast and efficient production of potential inhibitors against target biomolecules such as enzymes. Using this approach, complementary alkyne and azide building are assembled at binding sites and then accelerate the Huisgen 1,3-dipolar cycloaddition reaction to afford the corresponding conventional triazole, as illustrated in Fig. 1.

To date, *in situ* click chemistry research has garnered success in inhibitor explorations where acetylcholinester-

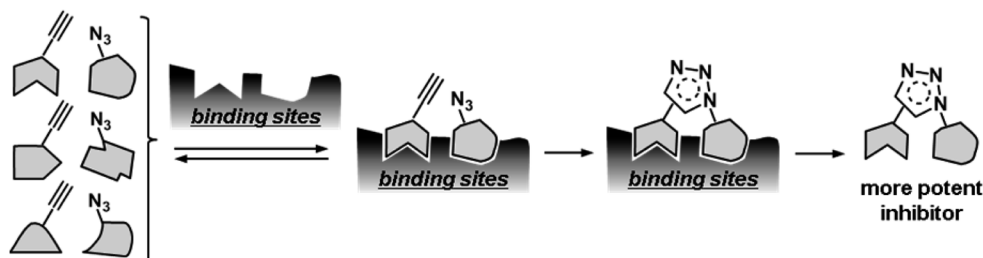


Fig. 1. Illustration of the *in Situ* Click Chemistry Strategy for Generating Modular Type Inhibitor

\* To whom correspondence should be addressed. e-mail: omuras@insti.kitasato-u.ac.jp; sunazuka@lisci.kitasato-u.ac.jp

ase,<sup>14–17</sup> carbonic anhydrase,<sup>18–21</sup> human immunodeficiency virus (HIV)-1 protease,<sup>22</sup> *Serratia marcescens* chitinase (*SmChi*),<sup>23–25</sup> *Mycobacterium tuberculosis* EthR protein,<sup>26</sup> Akt1,<sup>27</sup> acetylcholine binding protein,<sup>28</sup> G-Quadruplex<sup>29</sup> and biotin protein ligase inhibitors<sup>30</sup> have served as templates. Here, we report *in situ* click chemistry approaches, focusing on hDAO as the target enzyme to generate novel hDAO inhibitors.

## Results and Discussion

**Design of the Anchor Molecule** X-Ray analysis of hDAO/ligand co-crystals has identified several ligand molecules that inhibit hDAO activity by blocking the binding site of D-amino acids.<sup>31–35</sup> Of these structures, the complex of imino-3,4-dihydroxyphenylalanine (DOPA) bound to hDAO provides the best option for the design of an anchor molecule for using *in situ* click chemistry screening. Specifically, our aim was to generate azide- or alkyne-bearing derivatives of the imino-DOPA ligand molecule. As mentioned previously, the binding mode of imino-DOPA with hDAO has been significantly clarified by X-ray co-crystal analysis<sup>35–37</sup> (Fig. 2A). Our strategy was to generate candidate anchor molecules by introducing the alkyne function onto the nitrogen of imino-DOPA or imino-tyrosine, and onto methylated analogues (Fig. 2B).

**Preparation of the Alkyne-Bearing Anchor Molecules** The alkyne bearing derivatives were initially synthesized as

reactive scaffolds for capturing complementary azide compounds to generate triazole-linked inhibitors by target-guided synthesis (TGS) from two kinds of  $\alpha$ -keto acids (**1**, **2**<sup>38</sup>). Although imino-DOPA is known to be a good substrate to block at the active site of hDAO, the imine is normally recognized as a reactive function, which can be readily hydrolyzed in aqueous media to yield the corresponding ketone and amine. We therefore used oxime as an alternative functional group instead of the imine (Chart 1). The oxime formation of 4-hydroxyphenylpyruvic acid (**1**) with *O*-propargyl hydroxylamine (**3**) proceeded smoothly to give the corresponding *O*-propargyl oximes (**4a**) in 64% yield together with its methyl ester (**4b**) in 28% yield as single geometrical isomers, respectively, after silica gel column chromatography separation. Similarly, 3,4-dihydroxyphenylpyruvic acid (**2**) was converted to **5a** in 50% yield and **5b** in 24% yield, respectively. Further, *O*-alkylated analogues of phenolic alcohols from **4b** and **5b** were carried out by the methylation with dimethyl sulfate and potassium carbonate, furnishing the corresponding **6** in 81% yield and **7** in 77% yield, respectively.

The inhibitory activities of these anchor candidates towards hDAO were determined using an *in vitro* assay. hDAO catalyzes the oxidative deamination reaction of D-amino acids to  $\alpha$ -keto acids as follows;  $R-CH(NH_2)-COOH + O_2 + H_2O \rightarrow R-CO-COOH + NH_3 + H_2O_2$ . A colorimetric screen for detection of concentration of hydrogen peroxide ( $H_2O_2$ ) has been known

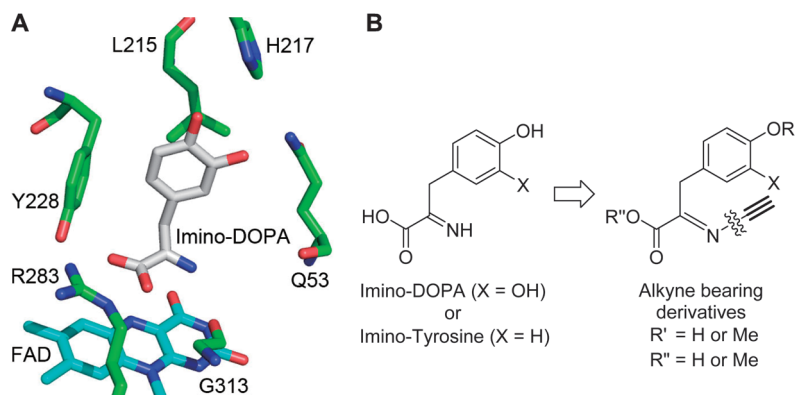


Fig. 2. Design of the Anchor Molecule

(A) The X-ray crystallographic structures of hDAO complexed with imino-DOPA (PDB ID: 2E82) shows imino-DOPA bound in the active site. (B) Alkyne-bearing derivatives designed based on the structure of the imino-DOPA framework.

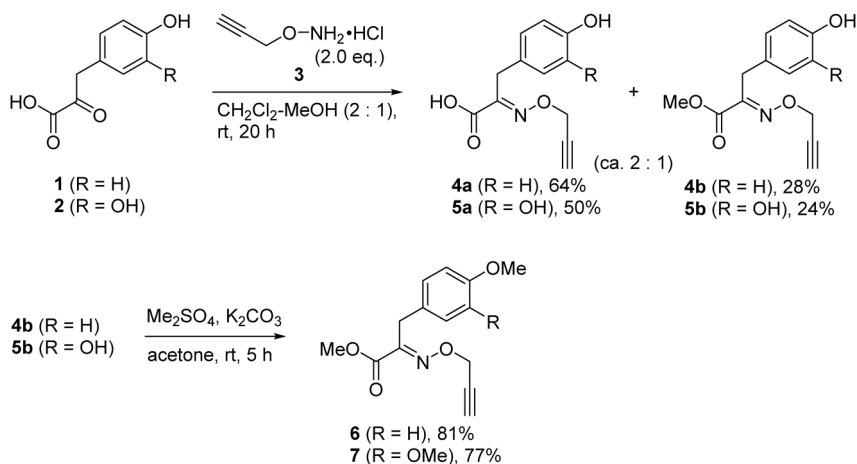


Chart 1. Synthesis of the Candidate Anchor Molecule

as a high-throughput method to evaluate oxidoreductases activities, which can be monitored by the green dye converted from the reaction of generated  $H_2O_2$  with a horseradish peroxidase (HRP)/2,2'-azino-bis(3-ethylbenzothiazoline)-6-sulfonic acid (ABTS).<sup>39</sup> Advantage of  $H_2O_2$ /ABTS/HRP assay is that the resulting green dye is relatively stable once oxidized. Although it has been reported that ABTS may autoxidize and be unstable, and that the assay is not very sensitive,<sup>40</sup> it was employed here for the initial evaluation of hDAO inhibitors because of its utility as a high-throughput screening technique. The  $IC_{50}$  value for each anchor candidate was determined based on the activity of sodium benzoate as a standard hDAO inhibitor ( $IC_{50}=10\mu M$ ).<sup>40</sup> Promising candidates identified by the  $H_2O_2$ /ABTS/HRP assay were then evaluated with an oxygraphic assay using a Clark oxygen electrode that measures the amount of molecular oxygen ( $O_2$ ), this more sensitive assay allowed calculation of the inhibition constant ( $K_i$ ) of the selected candidates.<sup>37,41</sup> In addition, determination of inhibition pattern was confirmed by the use of sodium benzoate ( $K_i$ :  $7\mu M$ )<sup>37,41</sup> as a well known competitive inhibitor, which has ability to occupy the binding site of D-amino acid of hDAO.

DOPA-type derivatives (**2**, **5a**, **b**) ( $IC_{50}$ :  $1.1$ – $7.3\mu M$ ) exhibited potent inhibitory activity compared with tyrosine-type derivatives (**1**, **4a**, **b**) ( $IC_{50}$ :  $11.7$ – $33.7\mu M$ ) (Table 1, first screening) using the  $H_2O_2$ /ABTS/HRP assay method, whereas the methoxyphenyl derivative **6** and **7** showed no activity. According to results of  $H_2O_2$ /ABTS/HRP assay, the promising four compounds (**4a**, **b**, **5a**, **b**) other than  $\alpha$ -keto acids (**1**, **2**) were tested using the oxygraphic assay to see whether the binding could be equipped to a level that would make a sufficiently good anchor at the active site, to be used for the capture of azide-bearing candidates through *in situ* triazole formation. The tyrosine-type derivatives **4a** and **b** were identified as potent competitive inhibitors with  $K_i$  values of 2.5 and 2.2 mM, respectively (Table 1, second screening). In contrast, the DOPA-type derivatives **5a** and **b** for inhibitory activity of hDAO was not confirmed and found to be weak obstructers of hDAO activity in noncompetitive inhibition pattern. It may cause that **5a** and **b** oneself became the reducer and consumed the  $H_2O_2$  oxidant, leading to their erroneous identification as strong hDAO inhibitors on  $H_2O_2$ /ABTS/HRP assay system. We therefore chose alkyne **4a**, which has better solubility into the aqueous media than that of **4b**, as a target “anchor molecule” for *in situ* click chemistry.

#### Screening for hDAO-Templated Reactions *In situ* click

Table 1. Results of the  $H_2O_2$ /ABTS/HRP and Oxygraphic Assays

Compounds	Anchor molecule types	First screening <sup>a)</sup> $IC_{50}$ ( $\mu M$ )	Second screening <sup>b)</sup> $K_i$ (mM)	Inhibition pattern with sodium benzoate
<b>1</b>		18.9	$\infty$	—
<b>4a</b>	Tyrosine-	33.7	2.5	Competitive
<b>4b</b>	type	11.7	2.2	Competitive
<b>6</b>		>300	—	—
<hr/>				
<b>2</b>		3.4	1.8	—
<b>5a</b>	DOPA-type	7.3	$\infty$	Non-competitive
<b>5b</b>		1.1	$\infty$	Non-competitive
<b>7</b>		>300	—	—

a)  $IC_{50}$  values were calculated by  $H_2O_2$ /ABTS/HRP assay. b)  $K_i$  values were calculated by oxygraphic assay.

chemistry screening was realized in parallel in 96-well microtiter plates to explore the hDAO accelerated triazole formation. Consequently, the alkyne anchor molecule **4a** ( $500\mu M$ ) and 250 structurally diverse azides ( $500\mu M$ ) were incubated in the presence of hDAO ( $2\mu M$ ) in 10% methanol containing phosphate buffer solution at pH 8.0 (Chart 2). The formation of the triazole products was monitored by HPLC and mass spectrometry using selected ion recording (SIR) detection (LC/MS-SIR) after 24 h at  $25^\circ C$ . After analysis of each reaction mixture, only azide **8**<sup>42</sup> was sufficiently accelerated in its cycloaddition with alkyne **4a** in the presence of the hDAO enzymes to yield a detectable amount of triazole **9** (at this point not distinguished as to whether a *syn*- and/or *anti*-substituted triazole) in the background with great reproducibility by LC/MS-SIR measurement (Fig. 3).

**Preparations and Determination of Hit Triazole** We turned our attention to distinguish the accelerated triazole as to whether an *anti* and/or *syn*-triazole by the template effect

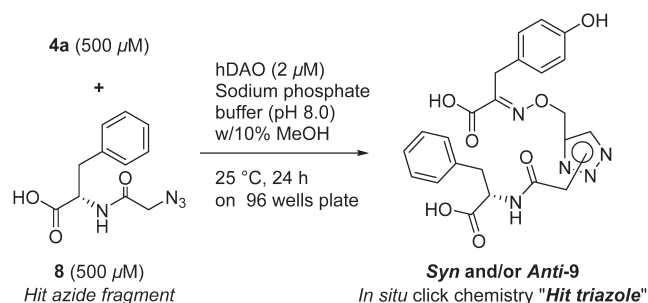


Chart 2. hDAO Template *In Situ* Click Chemistry Protocol Using an Anchor Alkyne Molecule (**4a**) and the Guided Analogue

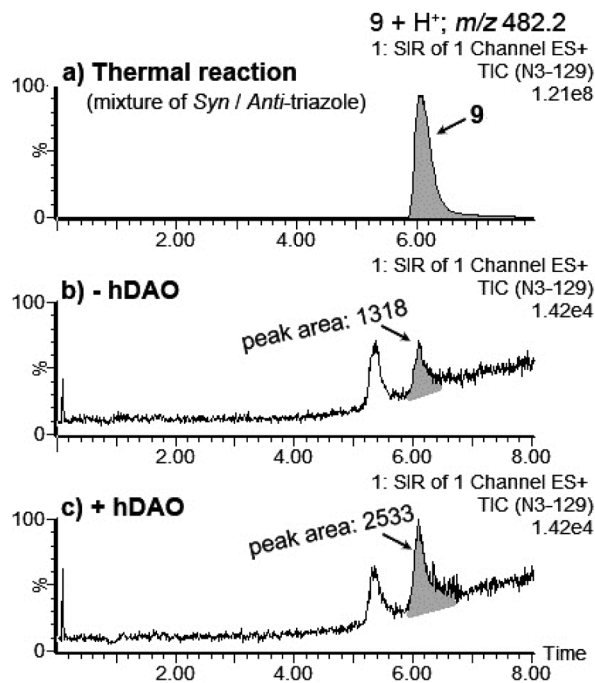
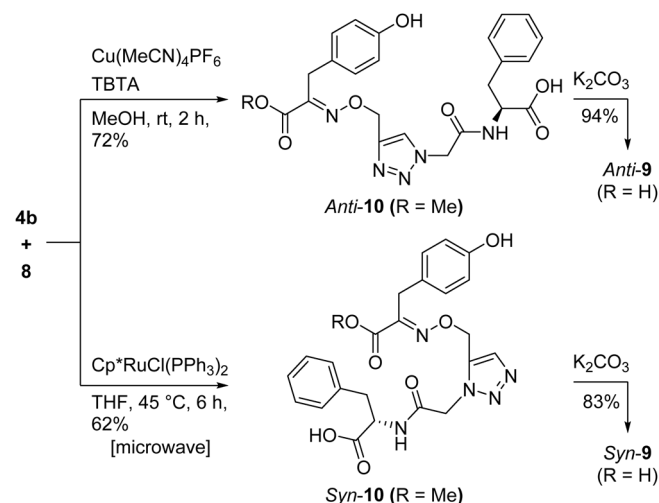


Fig. 3. Results of *In Situ* Click Chemistry between **4a** and **8** to Form Triazole **9**, Monitored by LC/MS-SIR

a) Authentic sample of *syn/anti* mixture of **9**<sup>43</sup> from thermal reaction ( $80^\circ C$ , 10h), apparently single peak (6.1 min) of **9** (*syn:anti*=1:1) was observed; b) Without hDAO (background reaction); c) Reaction between **4a** ( $500\mu M$ ) and **8** ( $500\mu M$ ) in the presence of hDAO ( $2\mu M$ ).

of hDAO. Therefore, alkyne **4b** and azide **8** were subjected to copper(I)-catalyzed azide-alkyne cycloaddition conditions (CuAAC),<sup>10,11</sup> along with the ruthenium-catalyzed azide-alkyne cycloaddition reaction conditions (RuAAC),<sup>12,13</sup> to prepare each pure positional isomers of **9**, thus allowing identification of the selectivity of the hDAO-guided triazole formation. Attempts of both triazole formations using substrate **4a** were unsuccessful, suggesting that the neighboring two functions, carboxylic acid and oxime in **4a** may suppress the cyclization reaction by chelating the metal catalysts. Therefore, the triazole formation was performed using the ester



TBTA=tris(benzyltriazolylmethyl)amine, THF=tetrahydrofuran.

Chart 3. Synthesis of *syn*- and *anti*-Triazole **9**

substrate **4b** with azide **8** to give the *anti*-**10** in 72% yield and *syn*-**10** in 62% yield as single isomers, respectively. Each isomer of **10** was then subjected to further hydrolysis under basic conditions to afford both *anti*- and *syn*-**9** in 94 and 83% yields, respectively (Chart 3).

Analysis of *syn* and/or *anti* selection for the *in situ* screening by optimized LC/MS-SIR detection revealed that a combination of alkyne **4a** and azide **8** had led to the accelerated the formation of *syn*-**9** in the presence of hDAO (Fig. 4). Interestingly, the triazole formation of an alternative isomer, *anti*-**9**, seems to be not accelerated under the condition of the *in situ* screening. The inhibitory activity of *syn*-**9**, hit compound of *in situ* screening, displayed high inhibitory activity of hDAO with  $K_i$  value of 0.5 mM in competitive inhibition pattern with sodium benzoate, measured by oxygraphic assay (Table 2). Azide compound (**8**) was unexpectedly found to be a potent inhibitor of hDAO, with a  $K_i$  value of 1.0 mM, but *syn*-**9** exhibited higher potency against hDAO than that of both azide and alkyne building blocks. On the other hand, an alternative isomer, *anti*-**9**, did not show the activity in competitive inhibition pattern (data not shown). The anchor molecule **4a** and azide substrate **8** functionalities present in *syn*-**9** make it a more potent inhibitor of hDAO compared to the parent compounds

Table 2.  $K_i$  Values for Hit Triazole *syn*-**9**, Azide **8** and Alkyne **4a**

Compounds	Inhibition pattern with sodium benzoate	$K_i$ (mM) <sup>a)</sup>
<i>syn</i> - <b>9</b>	Competitive	0.5
<b>8</b>	Competitive	1.0
<b>4a</b>	Competitive	2.5

a) Inhibition constant ( $K_i$ ) was calculated by oxygraphic assay.

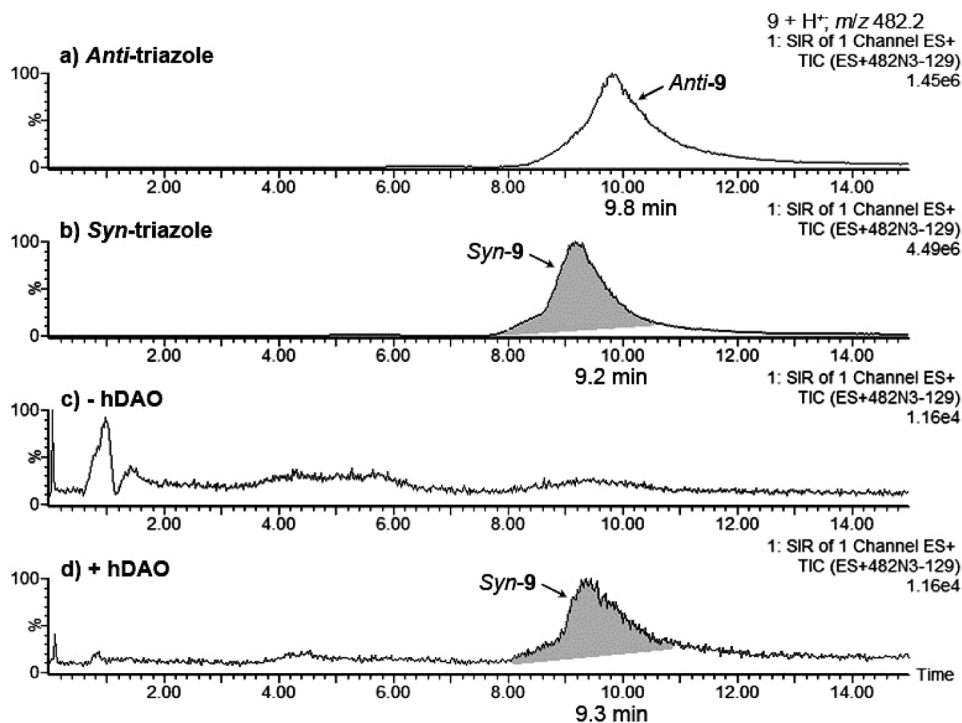


Fig. 4. Results of *in Situ* Click Chemistry between **4b** and **8** to Form Triazole **9**, as Monitored by LC/MS-SIR

Two possible isomers of the triazole were determined by isocratic separation analysis. a) Authentic sample of *anti* of **9** from chemical synthesis, was observed as a single peak (9.8 min); b) authentic sample of *syn* of **9** from chemical synthesis, was observed as a single peak (9.2 min); c) without hDAO (background reaction); d) preferentially generated *syn*-triazole **9** peak (9.3 min) by *in situ* click chemistry.

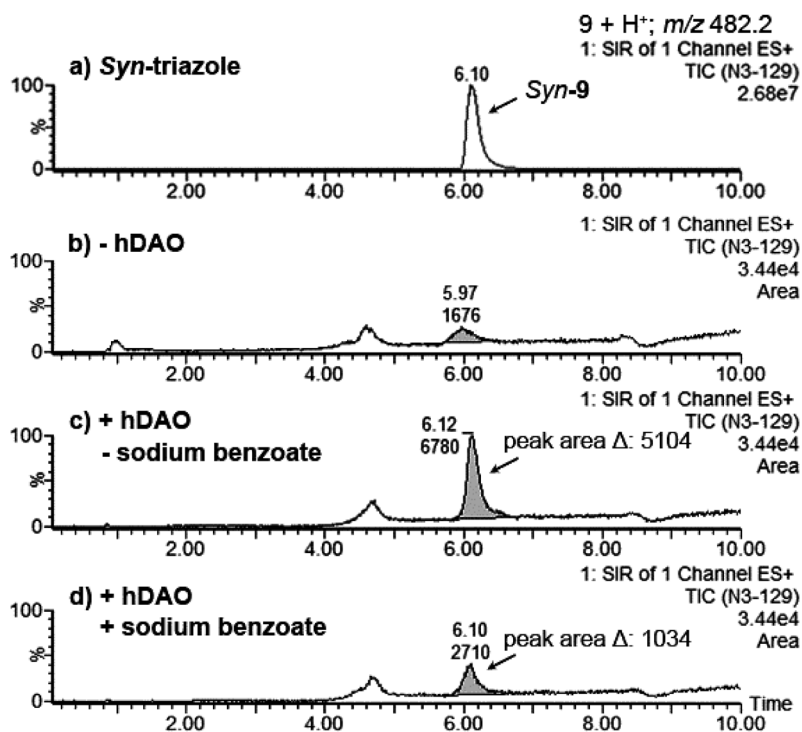


Fig. 5. Confirmation of the Template Effect of hDAO to Generate Triazole 9

a) Authentic sample of *syn-9*, single peak (6.1 min) was observed; b) without hDAO (background reaction); c) observation of *in situ* click chemistry of alkyne **4a** (500  $\mu$ M) and azide **8** (500  $\mu$ M) with hDAO; d) confirmation of competitive inhibition of the sodium benzoate (500  $\mu$ M) for *in situ* click chemistry.

and suggest it would be a highly specific antagonist against hDAO than **4a** and **8**.

#### Template Effect of hDAO in the Generation of *syn-9*

Having confirmed the selective formation of *syn-9* with hDAO, we next tried to observe the acceleration of triazole formation by the template effect at the binding site of amino acid in hDAO to guide *syn-9*. Analysis of *in situ* click chemistry focusing on between **4a** and **8** by the optimized LC/MS-SIR condition, which was modified to increase the sensitivity against compound *syn-9* based on the condition of Fig. 3, was performed. Significant suppression of the triazole formation **9** was observed in the control incubation containing hDAO and the same azide (500  $\mu$ M) and alkyne (500  $\mu$ M) in the presence of sodium benzoate (500  $\mu$ M) as a potent hDAO inhibitor ( $K_i$  value of hDAO: 7  $\mu$ M)<sup>37,41</sup> (Fig. 5, condition d), compared with condition b (background reaction) and condition c (*in situ* reaction) shown in Fig. 5. These results confirmed that the validating triazole **9** (among two possible isomers, *syn-9* was confirmed as a *in situ* guided compound in Fig. 4) was a hit compound and that its formation required access to the hDAO active site.

#### Conclusion

This article introduced *in situ* click chemistry approaches related to D-amino acid oxidase (DAO) as the target enzyme to generate novel and more potent DAO inhibitor. The strategy employed an alkyne function appended to an active domain, whose design was based on the X-ray co-crystal structure of hDAO and imino-DOPA. hDAO performed as a mold for triazole formation between an alkyne anchor molecule and selected azide fragment. In this process of *in situ* click chemistry, the highly exergonic nature of triazole formation makes process irreversible, and thereby locks in unique information

of ligand affinity site of enzyme. In effect, hDAO acted as a reaction vessel of molecular scale to create its own enhanced inhibitor and demonstrated the effectiveness of the target enzyme as a “casting mold.” *In situ* click chemistry protocol allowed us to discover a lead compound for discovery of an attractive hDAO inhibitor directed toward the functions of hDAO, without need for long and costly analog syntheses. Ongoing studies are directed toward optimizing the lead compound and further evaluating the bioactivities of hDAO inhibitors as potential therapeutics for diseases related to hDAO disorders.

#### Experimental

**General Information** hDAO was expressed in *Escherichia coli* and purified as previously reported.<sup>37</sup> All reagents were used as purchased without further purification unless otherwise noted. Unless otherwise noted, all reactions were carried out under nitrogen atmosphere. Precoated silica gel plates with a fluorescent indicator (Merck Ltd., Tokyo, Japan, 60 F254) were used for analytical and preparative thin layer chromatography. Flash column chromatography was carried out with Kanto Chemical silica gel (Kanto Chemical Co., Inc., Tokyo, Japan, Silica gel 60N, spherical neutral, 0.040–0.050 mm, catalog no. 37563-84) or Merck silica gel 230–400 mesh ASTM (Merck Ltd., Tokyo, Japan, 60N, 0.040–0.063 mm, catalog No. 109385). Microwave irradiation was carried out with Initiator +™ Eight (Biotage, Uppsala, Sweden). <sup>1</sup>H-NMR spectra were recorded at 500 MHz, and <sup>13</sup>C-NMR spectra were recorded at 125 MHz on JEOL ECA-500 (500 MHz) (JEOL Ltd., Tokyo, Japan). The chemical shifts are expressed in ppm downfield from internal solvent peaks CD<sub>3</sub>OD (3.31, 4.84 ppm, <sup>1</sup>H-NMR), CD<sub>3</sub>OD (49.0 ppm, <sup>13</sup>C-NMR), and *J* values are given in hertz. The coupling patterns are expressed by s (singlet), brs (broad

singlet), d (doublet), dd (double doublet), t (triplet), or m (multiplet). All infrared (IR) spectra were measured with a Horiba FT-210 spectrometer (HORIBA Ltd., Kyoto, Japan) spectrometer and were reported in wavenumbers ( $\text{cm}^{-1}$ ). High resolution (HR)-MS were measured on a JEOL JMS-700 MStation and JEOL JMS-T100LP (JEOL Ltd., Tokyo, Japan). Melting points were measured on a Yanaco micro melting system MP-500P (Yanaco New Science Inc., Kyoto, Japan). HPLC analysis was performed on a Waters 2795 separation module with Alliance HT (Nihon Waters K. K., Tokyo, Japan) equipped with a diode-array detector and micromass ZQ (Nihon Waters K. K., Tokyo, Japan).

**(E)-3-(4-Hydroxyphenyl)-2-[(2-propyn-1-yloxy)imino]propanoic Acid (4a) and Methyl (E)-3-(4-Hydroxyphenyl)-2-[(2-propyn-1-yloxy)imino]propanoate (4b)** To a solution of 4-hydroxyphenylpyruvic acid (**1**) (500 mg, 2.8 mmol) in  $\text{CH}_2\text{Cl}_2$ -MeOH (2:1 v/v) (28 mL) was added **3** (602 mg, 5.6 mmol) at room temperature. After stirring for 20 h, the reaction mixture was concentrated, and the residue was purified by flash column chromatography ( $\text{CHCl}_3$ -MeOH=50:1 to 10:1) to selectively afford (*E*)-oxime<sup>44</sup> (**4a**) (420 mg, 64%) as a colorless powder and (*E*)-oxime-methyl ester (**4b**) (194 mg, 28%) as a colorless powder, respectively (Chart 4). For **4a**: mp 137–139°C; IR (KBr)  $\nu_{\text{max}}$  ( $\text{cm}^{-1}$ ): 3487, 3255, 2121, 1712, 1604, 1512, 1435, 1357, 1257, 1219, 1126;  $^1\text{H-NMR}$  (500 MHz,  $\text{CD}_3\text{OD}$ )  $\delta$  (ppm): 7.08 (d, 2H,  $J=8.6$  Hz), 6.67 (d, 2H,  $J=8.6$  Hz), 4.86 (2H, d,  $J=2.3$  Hz), 3.80 (2H, s), 2.97 (1H, t,  $J=2.3$  Hz);  $^{13}\text{C-NMR}$  (125 MHz,  $\text{CD}_3\text{OD}$ )  $\delta$  (ppm): 165.8, 157.2, 153.9, 131.1 (2C), 127.7, 116.2 (2C), 79.7, 76.9, 63.7, 31.0; HR-MS (electrospray ionization (ESI))  $m/z$ : 256.0575  $[\text{M}+\text{Na}]^+$ ; Calcd for  $\text{C}_{12}\text{H}_{11}\text{NO}_4\text{Na}$ , 256.0580. For **4b**: mp 79–82°C; IR (KBr)  $\nu_{\text{max}}$  ( $\text{cm}^{-1}$ ): 3433, 3278, 2121, 1728, 1604, 1512, 1442, 1365, 1326, 1227, 1134;  $^1\text{H-NMR}$  (500 MHz,  $\text{CD}_3\text{OD}$ )  $\delta$  (ppm): 7.06 (d, 2H,  $J=8.4$  Hz), 6.67 (d, 2H,  $J=8.4$  Hz), 4.85 (2H, d,  $J=2.3$  Hz), 3.82 (2H, s), 3.78 (3H, s), 2.97 (1H, t,  $J=2.3$  Hz);  $^{13}\text{C-NMR}$  (125 MHz,  $\text{CD}_3\text{OD}$ )  $\delta$  (ppm): 165.0, 157.2, 153.4, 131.1 (2C), 127.5, 116.2 (2C), 79.7, 76.9, 63.8, 53.0, 31.2; HR-MS (ESI)  $m/z$ : 270.0732  $[\text{M}+\text{Na}]^+$ ; Calcd for  $\text{C}_{13}\text{H}_{13}\text{NO}_4\text{Na}$ , 270.0737.

**(E)-3-(3,4-Dihydroxyphenyl)-2-[(2-propyn-1-yloxy)imino]propanoic Acid (5a) and Methyl (E)-3-(3,4-Dihydroxyphenyl)-2-[(2-propyn-1-yloxy)imino]propanoate (5b)** According to the synthesis of **4a** and **b**, **2** (100 mg, 0.51 mmol) was selectively converted to (*E*)-oxime<sup>44</sup> **5a** (63.5 mg, 50%) as a colorless powder and (*E*)-oxime-methyl

ester **5b** (31.6 mg, 24%) as a colorless powder, respectively (Chart 5). For **5a**: mp 140–143°C; IR (KBr)  $\nu_{\text{max}}$  ( $\text{cm}^{-1}$ ): 3394, 3278, 2121, 1728, 1612, 1520, 1442, 1357, 1203, 1119;  $^1\text{H-NMR}$  (500 MHz,  $\text{CD}_3\text{OD}$ )  $\delta$  (ppm): 6.73 (1H, brs), 6.73 (d, 1H,  $J=8.1$  Hz), 6.59 (brd, 1H,  $J=8.1$  Hz), 4.80 (2H, brs), 3.80 (2H, s), 2.92 (1H, t,  $J=2.3$  Hz);  $^{13}\text{C-NMR}$  (125 MHz,  $\text{CD}_3\text{OD}$ )  $\delta$  (ppm): 170.2, 158.4, 146.1, 144.8, 129.0, 121.6, 117.4, 116.1, 80.2, 76.5, 63.0, 31.7; HR-MS (ESI)  $m/z$ : 272.0522  $[\text{M}+\text{Na}]^+$ ; Calcd for  $\text{C}_{12}\text{H}_{11}\text{NO}_5\text{Na}$ , 272.0529. For **5b**: mp 82–85°C; IR (KBr)  $\nu_{\text{max}}$  ( $\text{cm}^{-1}$ ): 3494, 3278, 2121, 1728, 1612, 1520, 1442, 1357, 1203, 1119;  $^1\text{H-NMR}$  (500 MHz,  $\text{CD}_3\text{OD}$ )  $\delta$  (ppm): 6.68 (1H, d,  $J=2.3$  Hz), 6.64 (1H, d,  $J=8.0$  Hz), 6.56 (1H, dd,  $J=8.0$ , 2.3 Hz), 4.85 (2H, d,  $J=2.3$  Hz), 3.78 (3H, s), 3.77 (2H, s), 2.96 (1H, t,  $J=2.3$  Hz);  $^{13}\text{C-NMR}$  (125 MHz,  $\text{CD}_3\text{OD}$ )  $\delta$  (ppm): 165.1, 153.5, 146.3, 145.1, 128.1, 121.4, 117.2, 116.3, 79.7, 76.9, 63.8, 53.0, 31.3; HR-MS (ESI)  $m/z$ : 286.0689  $[\text{M}+\text{Na}]^+$ ; Calcd for  $\text{C}_{13}\text{H}_{13}\text{NO}_5\text{Na}$ , 286.0686.

**Methyl (E)-3-(4-Methoxyphenyl)-2-[(2-propyn-1-yloxy)imino]propanoate (6)** To a solution of **4b** (30 mg, 0.12 mmol) in acetone (1 mL) were added dimethyl sulfate (19.0  $\mu\text{L}$ , 0.2 mmol) and potassium carbonate (69.1 mg, 0.5 mmol) at room temperature. After stirring for 5 h, the reaction was quenched by the addition of sat. aq.  $\text{NH}_4\text{Cl}$  (2 mL), and the resulting mixture was extracted with EtOAc (5 mL $\times$ 3). The combined organic layers were washed with brine (100 mL), dried over  $\text{Na}_2\text{SO}_4$  and concentrated. The residue was purified by flash column chromatography ( $\text{CHCl}_3$ -MeOH=50:1) to afford methyl ether (**6**) (25.6 mg, 81%) as a colorless oil. IR (KBr)  $\nu_{\text{max}}$  ( $\text{cm}^{-1}$ ): 3286, 2126, 1728, 1612, 1511, 1442, 1350, 1249, 1211, 1126;  $^1\text{H-NMR}$  (500 MHz,  $\text{CD}_3\text{OD}$ )  $\delta$  (ppm): 7.16 (2H, d,  $J=8.8$  Hz), 6.81 (2H, d,  $J=8.8$  Hz), 4.86 (2H, d,  $J=2.4$  Hz), 3.85 (2H, s), 3.78 (3H, s), 3.75 (3H, s), 2.97 (1H, t,  $J=2.3$  Hz);  $^{13}\text{C-NMR}$  (125 MHz,  $\text{CD}_3\text{OD}$ )  $\delta$  (ppm): 165.0, 160.0, 153.3, 131.1 (2C), 128.8, 114.9 (2C), 79.7, 77.0, 63.9, 55.6, 53.0, 31.2. HR-MS (FAB, 3-nitrobenzyl alcohol (NBA))  $m/z$ : 284.0898  $[\text{M}+\text{Na}]^+$ ; Calcd for  $\text{C}_{14}\text{H}_{15}\text{NO}_4\text{Na}$ , 284.0893.

**Methyl (E)-3-(3,4-dimethoxyphenyl)-2-[(2-propyn-1-yloxy)imino]propanoate (7)** According to the preparation of **6**, **5b** (30 mg, 0.11 mmol) was converted to **7** (25.6 mg, 77%) as a colorless oil; IR (KBr)  $\nu_{\text{max}}$  ( $\text{cm}^{-1}$ ): 3232, 2114, 1720, 1596, 1512, 1450, 1334, 1241, 1211, 1142;  $^1\text{H-NMR}$  (500 MHz,  $\text{CD}_3\text{OD}$ )  $\delta$  (ppm): 6.88 (1H, d,  $J=2.0$  Hz), 6.83 (1H, d,  $J=8.1$  Hz), 6.79 (1H, dd,  $J=8.1$ , 2.0 Hz), 4.88 (2H, d,  $J=2.3$  Hz), 4.86 (3H, s), 3.86 (2H, s), 3.80 (3H, s), 3.79 (6H, s), 3.00 (1H, t,  $J=2.3$  Hz);  $^{13}\text{C-NMR}$  (125 MHz,  $\text{CD}_3\text{OD}$ )  $\delta$  (ppm):

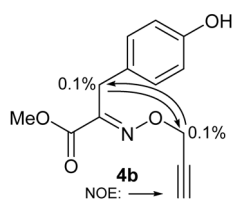
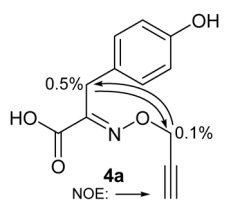


Chart 4

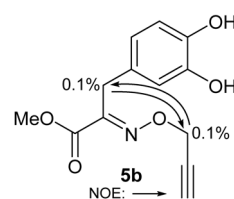
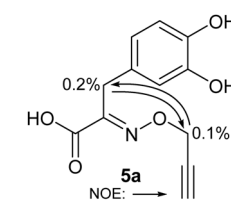


Chart 5

165.0, 153.1, 150.4, 149.4, 129.6, 122.5, 114.0, 113.1, 79.7, 77.0, 63.9, 56.5, 56.4, 53.1, 31.6; HR-MS (FAB, NBA)  $m/z$ : 314.0994  $[M+Na]^+$ ; Calcd for  $C_{15}H_{17}NO_3Na$ , 314.0999.

**(E)-4-[2-(4-Hydroxyphenyl)-1-methoxycarbonylethan-1-ylideneaminoxymethyl]-(1H-1,2,3-triazol-1-yl)acetyl-L-phenylalanine (Anti-10)** To a solution of alkyne **4b** (100.0 mg, 0.40 mmol) in MeOH (4 mL) were added  $Cu(MeCN)_4PF_6$  (15.0 mg, 0.04 mmol), tris(benzyltriazolylmethyl)amine (TBTA) (21.2 mg, 0.04 mmol) and azide **8** (89.4 mg, 0.36 mmol) at room temperature. After stirring for 2 h, the mixture was concentrated under reduced pressure. The residue was purified by flash column chromatography ( $CHCl_3$ -MeOH=10:1) to afford *anti-10* (128.8 mg, 72%) as a colorless powder.; mp 170–173°C; IR (KBr)  $\nu_{max}$  ( $cm^{-1}$ ): 3293, 2954, 2337, 1728, 1674, 1612, 1512, 1442, 1335, 1219, 1126;  $^1H$ -NMR (500 MHz,  $CD_3OD$ )  $\delta$  (ppm): 7.80 (1H, s), 7.26–7.14 (5H, m), 6.99 (2H, d,  $J=8.6$  Hz), 6.44 (2H, d,  $J=8.6$  Hz), 5.35 (2H, s), 5.12 (1H, d,  $J=16.0$  Hz), 5.09 (1H, d,  $J=16.0$  Hz), 4.63 (1H, dd,  $J=8.6, 4.6$  Hz), 3.78 (2H, s), 3.76 (3H, s), 3.24 (1H, dd,  $J=13.9, 4.6$  Hz), 2.98 (1H, dd,  $J=13.9, 8.6$  Hz);  $^{13}C$ -NMR (125 MHz,  $CD_3OD$ )  $\delta$  (ppm): 175.8, 167.1, 165.2, 157.2, 153.3, 144.6, 138.7, 131.1 (2C), 130.4 (2C), 129.4 (2C), 127.6, 127.1, 116.3 (2C), 69.2, 56.4, 53.1, 53.04, 53.00, 38.8, 31.2; HR-MS (ESI)  $m/z$ : 518.1646  $[M+Na]^+$ ; Calcd for  $C_{24}H_{25}N_5O_7Na$ , 518.1646.

**(E)-4-[2-(4-Hydroxyphenyl)-1-carboxylethan-1-ylideneaminoxymethyl]-(1H-1,2,3-triazol-1-yl)acetyl-L-phenylalanine (Anti-9)** *Anti-10* (50.0 mg, 0.10 mmol) was dissolved into the solution of  $K_2CO_3$  (13.8 mg, 0.10 mmol) in MeOH- $H_2O$  (2:1 v/v) (2 mL). The resulting mixture was stirred for 1 h at room temperature and then acidified by the addition of 1 M HCl aqueous solution (2 mL). The acidic solution was extracted with AcOEt (10 mL  $\times$  3), and the combined organic layers were dried over  $Na_2SO_4$  and concentrated to give pure product *anti-9* (45.3 mg, 94%) as a colorless powder.; mp 180–182°C; IR (KBr)  $\nu_{max}$  ( $cm^{-1}$ ): 3317, 3024, 2360, 1720, 1658, 1550, 1512, 1466, 1373, 1234, 1149;  $^1H$ -NMR (500 MHz,  $CD_3OD$ )  $\delta$  (ppm): 7.87 (1H, s), 7.27–7.16 (5H, m), 7.00 (2H, d,  $J=8.6$  Hz), 6.64 (2H, d,  $J=8.6$  Hz), 5.35 (2H, s), 5.16 (1H, d,  $J=16.0$  Hz), 5.11 (1H, d,  $J=16.0$  Hz), 4.71 (1H, dd,  $J=8.6, 4.6$  Hz), 3.77 (2H, s), 3.24 (1H, dd,  $J=14.0, 4.6$  Hz), 3.00 (1H, dd,  $J=14.0, 8.6$  Hz);  $^{13}C$ -NMR (125 MHz,  $CD_3OD$ )  $\delta$  (ppm): 174.1, 167.4, 166.0, 157.1, 153.7, 144.7, 138.1, 131.1 (2C), 130.3 (2C), 129.6 (2C), 127.9, 127.8, 127.3, 116.2 (2C), 69.0, 55.2, 53.0, 38.3, 31.0; HR-MS (ESI)  $m/z$ : 504.1483  $[M+Na]^+$ ; Calcd for  $C_{23}H_{23}N_5O_7Na$ , 504.1490.

**(E)-5-[2-(4-Hydroxyphenyl)-1-methoxycarbonylethan-1-ylideneaminoxymethyl]-(1H-1,2,3-triazol-1-yl)acetyl-L-phenylalanine (Syn-10)** To a solution of alkyne **4b** (100.0 mg, 0.4 mmol) in tetrahydrofuran (THF) (4 mL) were added  $Cp^*RuCl(PPh_3)_2$  (37.4 mg, 0.04 mmol) and azide **8** (89.5 mg, 0.36 mmol). The reaction mixture was heated to 45°C by the irradiation of microwave with strring. After 6 h, the reaction mixture was cooled to room temperature and concentrated under reduced pressure. The residue was purified by flash column chromatography ( $CHCl_3$ -MeOH=10:1) to afford *syn-10* (111.0 mg, 62%) as a colorless powder.; mp 80–83°C; IR (KBr)  $\nu_{max}$  ( $cm^{-1}$ ): 3302, 2954, 2337, 1728, 1674, 1612, 1511, 1442, 1365, 1211, 1119;  $^1H$ -NMR (500 MHz,  $CD_3OD$ )  $\delta$  (ppm): 7.69 (1H, s), 7.23–7.12 (5H, m), 6.96 (2H, d,  $J=8.6$  Hz), 6.66 (2H, d,  $J=8.6$  Hz), 5.25–5.22 (2H, complex

m; due to rotational isomers), 5.14–5.05 (2H, complex m; due to rotational isomers), 4.62 (1H, dd,  $J=8.0, 4.6$  Hz), 3.78 (3H, s), 3.76 (2H, s), 3.26 (1H, dd,  $J=13.8, 4.6$  Hz), 2.95 (1H, dd,  $J=13.8, 8.0$  Hz);  $^{13}C$ -NMR (125 MHz,  $CD_3OD$ )  $\delta$  (ppm): 176.1, 167.0, 164.9, 157.3, 153.8, 138.9, 136.2, 135.4, 131.0 (2C), 130.4 (2C), 129.4 (2C), 127.6, 127.5, 116.4 (2C), 65.4, 56.5, 53.2, 51.7, 39.0, 31.2; HR-MS (ESI)  $m/z$ : 518.1649  $[M+Na]^+$ ; Calcd for  $C_{24}H_{25}N_5O_7Na$ , 518.1652.

**(E)-5-[2-(4-Hydroxyphenyl)-1-carboxylethan-1-ylideneaminoxymethyl]-(1H-1,2,3-triazol-1-yl)acetyl-L-phenylalanine (Syn-9)** According to the synthesis of *anti-9*, *syn-10* (50.0 mg, 0.10 mmol) was converted to *syn-9* (40.0 mg, 83%) as a colorless powder.; mp 86–87°C; IR (KBr)  $\nu_{max}$  ( $cm^{-1}$ ): 3325, 2962, 2330, 1728, 1682, 1543, 1512, 1450, 1365, 1227, 1111;  $^1H$ -NMR (500 MHz,  $CD_3OD$ )  $\delta$  (ppm): 7.70 (1H, s), 7.27–7.16 (5H, m), 6.98 (2H, d,  $J=8.8$  Hz), 6.66 (2H, d,  $J=8.8$  Hz), 5.26–5.22 (2H, complex m; due to rotational isomers), 5.17–5.08 (2H, complex m; due to rotational isomers), 4.72 (1H, dd,  $J=9.2, 5.2$  Hz), 3.75 (2H, s), 3.24 (1H, dd,  $J=13.8, 5.2$  Hz), 2.96 (1H, dd,  $J=13.8, 9.2$  Hz);  $^{13}C$ -NMR (125 MHz,  $CD_3OD$ )  $\delta$  (ppm): 174.1, 167.4, 165.9, 157.2, 154.6, 138.1, 136.2, 135.4, 131.0 (2C), 130.3 (2C), 129.6 (2C), 127.9, 127.7, 116.3 (2C), 65.3, 55.2, 51.6, 38.5, 31.1; HR-MS (ESI)  $m/z$ : 504.1484  $[M+Na]^+$ ; Calcd for  $C_{23}H_{23}N_5O_7Na$ , 504.1490.

#### hDAO Activity Measurements

##### Protocol of $H_2O_2$ /ABTS/HRP Assay

To measure  $H_2O_2$  concentration, FAD (100  $\mu M$ ), compounds (1–300  $\mu M$ , 10% MeOH), 2,2-azinobis(3-ethylbenzthiazoline)-6-sulfonic acid (ABTS) (1 mM), hDAO (0.2  $\mu M$ ) and horseradish peroxidase (1 unit/mL) were added to 96 well micro plate. The increase in absorbance at 420 nm (Corona Electric, SH-9000 Lab) was monitored for 10 min after the addition of D-Proline (1 mM) at 25°C and compared with a calibration curve obtained with the known amounts of sodium benzoate.

##### Protocol of Oxygraphic Assay

hDAO activity was measured in oxygraphic assays (Oxygraph Plus, Hansatech, U.K.).<sup>37,41</sup> The standard reaction mixture contained D-Proline, hDAO and 20  $\mu M$  FAD, and hDAO inhibitor in a total volume of 2.0 mL. The reactions were initiated by the addition of hDAO and carried out in 0.1 M sodium phosphate buffer (pH 8.0) at 25°C. The Michaelis constant ( $K_m$ ) and turnover number ( $K_{cat}$ ) were estimated from double reciprocal plots of the initial velocity versus the substrate concentration. The inhibition constant ( $K_i$ ) for compound was estimated from Dixon plots<sup>45,46</sup> of the initial velocity versus the D-Proline concentration in the presence of benzoate (0–10  $\mu M$ ).

**Experiment for the Broad Screening *in Situ* Click Chemistry with hDAO** Alkyne **4a** (5  $\mu L$ ; 10.0 mM in MeOH) was diluted in 0.1 M sodium phosphate buffer (pH 8.0) (70  $\mu L$ ). Subsequently, the required FAD (10  $\mu L$ ; 100 mM in 0.1 M sodium phosphate buffer (pH 8.0)) and azide compound (5  $\mu L$ ; 10.0 mM in MeOH) were added to the alkyne solution, in 0.1 M sodium phosphate buffer to give final concentrations of 2.0  $\mu M$  hDAO, 500  $\mu M$  alkyne **4a** and 500  $\mu M$  of each azide in 10% MeOH/phosphate buffer (100  $\mu L$ ). After mixing thoroughly, the reaction mixtures were incubated at 25°C for 24 h, then diluted with 100  $\mu L$  MeOH to restrain the hDAO activity and injected directly into the LC/UV-MS instrument to perform LC/MS-SIR analysis: Conditions for HPLC; column, Senshu Pak Pegasil ODS SP100 (Senshu Scientific Co., Tokyo, Japan)

2×50 mm, gradient 10% MeCN (0.05% trifluoroacetic acid (TFA)) in H<sub>2</sub>O (0.1% TFA) to 100% MeCN (0.05% TFA) over 8 min, flow 0.3 mL min<sup>-1</sup>, detect 200–400 nm, temp 20°C; MS-SIR: cone voltage 40 V, source temp 110°C, desolvation temp 350°C, selected mass 482.2 [M+Na]<sup>+</sup>. The triazole products were identified by their retention times and molecular weights. Control experiments without hDAO, FAD (10 μL; 100 mM in 0.1 M sodium phosphate buffer (pH 8.0)) and alkyne **2** (5 μL; 10.0 mM in MeOH) and azides (5 μL; 10.0 mM in MeOH) in 0.1 M sodium phosphate buffer (pH 8.0) (80 μL) at 25°C for 24 h) were run consecutively.

**The Condition of LC/MS-SIR for Identification of the Hit Triazole Isomer** Column, DOCOSIL C22 (Senshu Scientific Co., Tokyo, Japan) 2φ×50 mm, isocratic 20% MeCN in H<sub>2</sub>O (0.08% HCOOH), flow 0.2 mL min<sup>-1</sup>, detect 210–400 nm, temp 20°C; MS-SIR: cone voltage 38 V, source temp 110°C, desolvation temp 350°C, selected mass 482.2 [M+Na]<sup>+</sup>.

**Experiment of *in Situ* Click Chemistry of Alkyne **4a** and Azide **8** with hDAO** The condition of hDAO template triazole formation was followed to the procedure of broad screening method of *in situ* click chemistry. The detection condition of triazole compound by MS-SIR was only optimized to increase its sensitivity as follows; cone voltage 38 V, source temp 110°C, desolvation temp 350°C, selected mass 482.2 [M+Na]<sup>+</sup>.

**Acknowledgments** This work was supported by a Grant from The Naito Foundation, Cooperative Research Grant of the Institute for Enzyme Research, Joint Usage/Research Center, Tokushima University, and a Kitasato University Research Grant for Young Researchers to T. H. We thank Dr. Kenichiro Nagai and Ms. Noriko Sato (School of Pharmacy, Kitasato University) for various instrumental analyses.

**Conflict of Interest** The authors declare no conflict of interest.

## References and Notes

- Park H. K., Shishido Y., Ichise-Shishido S., Kawazoe T., Ono K., Iwana S., Tomita Y., Yorita K., Sakai T., Fukui K., *J. Biochem.*, **139**, 295–304 (2006).
- Krebs H. A., *Biochem. J.*, **29**, 1620–1644 (1935).
- Javitt D. C., Zukin S. R., *Am. J. Psychiatry*, **148**, 1301–1308 (1991).
- Krystal J. H., Karper L. P., Seibyl J. P., Freeman G. K., Delaney R., Bremner J. D., Heninger G. R., Bowers M. B. Jr., Charney D. S., *Arch. Gen. Psychiatry*, **51**, 199–214 (1994).
- Chumakov I., Blumenfeld M., Guerassimenko O., Cavarec L., Palicio M., Abderrahim H., Bougueleret L., Barry C., Tanaka H., La Rosa P., Puech A., Tahri N., Cohen-Akenine A., Delabrosse S., Lissarrague S., Picard F.-P., Maurice K., Essieux L., Millasseau P., Grel P., Debailleul V., Simon A.-M., Caterina D., Dufaure I., Malekzadeh K., Belova M., Luan J.-J., Bouillot M., Sambucy J.-L., Primas G., Saumier M., Boubkiri N., Martin-Saumier S., Nasroune M., Peixoto H., Delaye A., Pinchot V., Bastucci M., Guillou S., Chevillon M., Sainz-Fuertes R., Meguenni S., Aurich-Costa J., Cherif D., Gimalac A., Van Duijn C., Gauvreau D., Ouellette G., Fortier I., Raelson J., Sherbatich T., Riazanskaia N., Rogaev E., Raeymaekers P., Aerssens J., Konings F., Luyten W., Macchiardi F., Sham P. C., Straub R. E., Weinberger D. R., Cohen N., Cohen D., *Proc. Natl. Acad. Sci. U.S.A.*, **99**, 13675–13680 (2002).
- Michael A., *J. Prakt. Chem.*, **48**, 94–95 (1893).
- Huisgen R., *Pure Appl. Chem.*, **61**, 613–628 (1989).
- Huisgen R., “1,3-Dipolar Cycloaddition Chemistry,” Vol. 1, ed. by Padwa A., Wiley, New York, 1984, pp. 1–176.
- Kolb H. C., Finn M. G., Sharpless K. B., *Angew. Chem. Int. Ed.*, **40**, 2004–2021 (2001).
- Rostovtsev V. V., Green L. G., Fokin V. V., Sharpless K. B., *Angew. Chem. Int. Ed.*, **41**, 2596–2599 (2002).
- Tornøe C. W., Christensen C., Meldal M., *J. Org. Chem.*, **67**, 3057–3064 (2002).
- Zhang L., Chen X., Xue P., Sun H. H. Y., Williams I. D., Sharpless K. B., Fokin V. V., Jia G., *J. Am. Chem. Soc.*, **127**, 15998–15999 (2005).
- Rasmussen L. K., Boren B. C., Fokin V. V., *Org. Lett.*, **9**, 5337–5339 (2007).
- Mamidyala S. K., Finn M. G., *Chem. Soc. Rev.*, **39**, 1252–1261 (2010).
- Lewis W. G., Green L. G., Grynszpan F., Radić Z., Carlier P. R., Taylor P., Finn M. G., Sharpless K. B., *Angew. Chem. Int. Ed.*, **41**, 1053–1057 (2002).
- Manetsch R., Krasinski A., Radić Z., Raushel J., Taylor P., Sharpless K. B., Kolb H. C., *J. Am. Chem. Soc.*, **126**, 12809–12818 (2004).
- Krasinski A., Radić Z., Manetsch R., Raushel J., Taylor P., Sharpless K. B., Kolb H. C., *J. Am. Chem. Soc.*, **127**, 6686–6692 (2005).
- Mocharla V. P., Colasson B., Lee L. V., Röper S., Sharpless K. B., Wong C.-H., Kolb H. C., *Angew. Chem. Int. Ed.*, **44**, 116–120 (2004).
- Wang J., Sui G., Mocharla V. P., Lin R. J., Phelps M. E., Kolb H. C., Tseng H.-R., *Angew. Chem. Int. Ed.*, **45**, 5276–5281 (2006).
- Wang Y., Lin W.-Y., Liu K., Lin R. J., Selke M., Kolb H. C., Zhang N., Zhao X.-Z., Phelps M. E., Shen C. K. F., Faull K. F., Tseng H.-R., *Lab. Chip.*, **9**, 2281–2285 (2009).
- Lee S. S., Lim J., Tan S., Cha J., Yeo S. Y., Agnew H. D., Heath J. R., *Anal. Chem.*, **82**, 672–679 (2010).
- Whiting M., Muldoon J., Lin Y.-C., Silverman S. M., Lindstrom W., Olson A. J., Kolb H. C., Finn M. G., Sharpless K. B., Elder J. H., Fokin V. V., *Angew. Chem. Int. Ed.*, **45**, 1435–1439 (2006).
- Hirose T., Sunazuka T., Sugawara A., Endo A., Iguchi K., Yamamoto T., Ui H., Shiomi K., Watanabe T., Sharpless K. B., Ōmura S., *J. Antibiot.*, **62**, 277–282 (2009).
- Hirose T., Sunazuka T., Ōmura S., *Proc. Jpn. Acad. Ser. B*, **86**, 85–102 (2010).
- Hirose T., Maita N., Gouda H., Koseki J., Yamamoto T., Sugawara A., Nakano H., Hirono S., Shiomi K., Watanabe T., Taniguchi H., Sharpless K. B., Ōmura S., Sunazuka T., *Proc. Natl. Acad. Sci. U.S.A.*, **110**, 15892–15897 (2013).
- Willand N., Desroses M., Toto P., Dirie B., Lens Z., Villeret V., Rucktooa P., Loch C., Baulard A., Deprez B., *ACS Chem. Biol.*, **5**, 1007–1013 (2010).
- Millward S. W., Henning R. K., Kwong G. A., Pitram S., Agnew H. D., Deyle K. M., Nag A., Hein J., Lee S. S., Lim J., Pfeilsticker J. A., Sharpless K. B., Heath J. R., *J. Am. Chem. Soc.*, **133**, 18280–18288 (2011).
- Grimster N. P., Stump B., Fotsing J. R., Weide T., Talley T. T., Yamauchi J. G., Nemezc Á., Kim C., Ho K.-Y., Sharpless K. B., Taylor P., Fokin V. V., *J. Am. Chem. Soc.*, **134**, 6732–6740 (2012).
- Di Antonio M., Biffi G., Mariani A., Raiber E.-A., Rodriguez R., Balasubramanian S., *Angew. Chem. Int. Ed.*, **51**, 11073–11078 (2012).
- Tieu W., Soares da Costa T. P., Yap M. Y., Keeling K. L., Wilce M. C. J., Wallace J. C., Booker G. W., Polyak S. W., Abell A. D., *Chem. Sci.*, **4**, 3533–3537 (2013).
- Sparey T., Abeywickrema P., Almond S., Brandon N., Byrne N., Campbell A., Hutson P. H., Jacobson M., Jones B., Munshi S., Pascarella D., Pike A., Prasad G. S., Sachs N., Sakatis M., Sardana V., Venkatraman S., Young M. B., *Bioorg. Med. Chem. Lett.*, **18**, 3386–3391 (2008).



- 32) Duplantier A. J., Becker S. L., Bohanon M. J., Borzilleri K. A., Chrunyk B. A., Downs J. T., Hu L.-Y., El-Kattan A., James L. C., Liu S., Lu J., Maklad N., Mansour M. N., Mente S., Piotrowski M. A., Sakya S. M., Sheehan S., Steyn S. J., Strick C. A., Williams V. A., Zhang L., *J. Med. Chem.*, **52**, 3576–3585 (2009).
- 33) Hondo T., Warizaya M., Niimi T., Namatame I., Yamaguchi T., Nakanishi K., Hamajima T., Harada K., Sakashita H., Matsumoto Y., Orita M., Takeuchi M., *J. Med. Chem.*, **56**, 3582–3592 (2013).
- 34) Hopkins S. C., Heffernan M. L. R., Saraswat L. D., Bowen C. A., Melnick L., Hardy L. W., Orsini M. A., Allen M. S., Koch P., Spear K. L., Foglesong R. J., Soukri M., Chytil M., Fang Q. K., Jones S. W., Varney M. A., Panatier A., Oliet S. H. R., Pollegioni L., Piubelli L., Molla G., Nardini M., Large T. H., *J. Med. Chem.*, **56**, 3710–3724 (2013).
- 35) Kawazoe T., Tsuge H., Imagawa T., Aki K., Kuramitsu S., Fukui K., *Biochem. Biophys. Res. Commun.*, **355**, 385–391 (2007).
- 36) Kawazoe T., Park H. K., Iwana S., Tsuge H., Fukui K., *Chem. Rec.*, **7**, 305–315 (2007).
- 37) Kawazoe T., Tsuge H., Pilone M. S., Fukui K., *Protein Sci.*, **15**, 2708–2717 (2006).
- 38) Wilson M. L., Coscia C. J., *J. Org. Chem.*, **44**, 301–302 (1979).
- 39) Gabler M., Hensel M., Fischer L., *Enzyme Microb. Tech.*, **27**, 605–611 (2000).
- 40) Nicell J. A., Bewtra J. K., Biswas N., St. Pierre C. C., Taylor K. E., *Can. J. Civ. Eng.*, **20**, 725–735 (1993).
- 41) Molla G., Sacchi S., Bernasconi M., Pilone M. S., Fukui K., Pollegioni L., *FEBS Lett.*, **580**, 2358–2364 (2006).
- 42) Aizpurua J. M., Azcune I., Fratila R. M., Balentova E., Sagartzazu-Aizpurua M., Miranda J. I., *Org. Lett.*, **12**, 1584–1587 (2010).
- 43) Preparation of authentic sample of mixture of *anti*- and *syn*-triazoles **9** (Thermal condition); A solution alkyne **4a** (5 mg, 0.021 mmol) and azide **8** (5.3 mg, 0.021 mmol) in MeOH (0.3 mL) was heated to 80°C, and stirred for 10 h. Then, the mixture (*anti*:*syn*=1:1) was direct analyzed by the LC/MS.
- 44) Hentschel F., Sasse F., Lindel T., *Org. Biomol. Chem.*, **10**, 7120–7133 (2012).
- 45) Dixon M., *J. Biochem.*, **55**, 170–171 (1953).
- 46) Dixon M., *J. Biochem.*, **129**, 197–202 (1972).